scientific reports

Check for updates

OPEN

Pantoea piersonii IIIF1SW-P2^T triggers cytotoxicity through L-asparaginase-driven ammonium secretion and colonizes reproductive tract of *Caenorhabditis elegans*

Asif Hameed[1,2]✉, Chiu-Chung Young[3,4,5]✉, Kokkarambath Vannadil Suchithra[1], Ashwini Prabhu[6], Honagodu Ravichandra Dhanyashree[1,2] & Rajesh Padumane Shastry[1,2]✉

Pantoea piersonii **IIIF1SW-P2^T (basionym *Kalamiella piersonii* IIIF1SW-P2^T), a bacterial species isolated from the International Space Station, was predicted to be non-pathogenic to humans, unlike its clinical counterpart *P. piersonii* YU22, which induces struvite crystallization and causes toxicity to Human Embryonic Kidney cell line (HEK 293 T). Here, we identify L-asparaginase-mediated cytotoxicity of IIIF1SW-P2^T on HEK 293 T *in vitro* and demonstrate strain's colonization ability in the reproductive tract *in vivo* using *Caenorhabditis elegans* as a model system. The recombinant L-asparaginase of IIIF1SW-P2^T (Kp_AnsA, ~ 37 kDa) generated significant amounts of NH_4^+ (4.1–15.5 µM, $P < 0.0001$) and exerted cytotoxicity to HEK 293 T (29.1–36.0%, $P < 0.0001$). NH_4^+-driven cytotoxicity of HEK 293 T was validated through the introduction of nearly equimolar amounts of standard NH_4^+ (12.7 µM; 31% cytotoxicity, $P < 0.0001$). Kp_AnsA found to be a halotolerant enzyme, highly active in alkaline pH (optimum pH 9), and exhibited K_m, V_{max} and K_{cat} values of 5.4 mM, 8.4 U/mg and 135.6 µmoles s^{-1}, respectively, in the presence of L-asparagine. Kp_AnsA displayed absolute amino acid sequence identity with that of YU22 and formed a tight phyletic association with that of marine bacteria. Analysis *in vivo* revealed the rapid and sustained colonization of green fluorescent protein (*gfp*)-tagged IIIF1SW-P2^T in the reproductive tract with 5% mortality of *C. elegans*. *Gfp*-tagged IIIF1SW-P2^T were localized at the vulvar and luminal regions, embryos and interembryonic space of *C. elegans*. The role of L-asparaginase in the colonization of IIIF1SW-P2^T at the reproductive tract of *C. elegans* merits further investigation. Nonetheless, this study demonstrated cytotoxicity of bacterial L-asparaginase on HEK 293 T and discovered the potential ability of IIIF1SW-P2^T to colonize the reproductive tract of a eukaryote.**

Keywords Amino acid catabolism, Virulence, Drug resistance, Cytotoxicity, Lithogenesis, Colonization, International Space Station

Abbreviations

ANOVA	Analysis of variance

[1]Division of Microbiology and Biotechnology, Yenepoya Research Centre, Yenepoya (Deemed to Be University), Deralakatte, Mangalore 575018, India. [2]Caenorhabditis elegans Laboratoy Facility (CeLF), Yenepoya Research Centre, Yenepoya (Deemed to Be University), Deralakatte, Mangalore 575018, India. [3]Department of Soil and Environmental Sciences, College of Agriculture and Natural Resources, National Chung Hsing University, Taichung 402, Taiwan. [4]Tetanti AgriBiotech Inc, No. 1, Gongyequ 10Th Rd, Xitun Dist, Taichung 40755, Taiwan. [5]Innovation and Development Center of Sustainable Agriculture, National Chung Hsing, University, Taichung 402, Taiwan. [6]Division of CART, Yenepoya Research Centre, Yenepoya (Deemed to Be University), Deralakatte, Mangalore 575018, India. ✉email: asifhameed@yenepoya.edu.in; ccyoung@mail.nchu.edu.tw; rpshastry@yenepoya.edu.in

AO-EB	Acridine orange-ethidium bromide
BL21 (DE3)	*E. coli* BL21 (DE3)
BLASTp	Basic local alignment search tool for protein
CFU	Colony-forming units
CLM	Cell line media
CLMA	CLM supplemented with L-asparagine
CLM_Kp_AnsA	CLM containing Kp_AnsA
CLMA_Kp_AnsA	CLMA containing Kp_AnsA
CLM_NH_4OH	CLM containing aqueous NH_4OH
DH5α	*E. coli* DH5α
gDNA	Genomic DNA
GBWT	Gehan-breslow-wilcoxon test
Gfp	Green fluorescent protein
HEK 293 T	Human embryonic kidney cell line
IIIF1SW-$P2^T$	Wild-type *Pantoea piersonii* IIIF1SW-$P2^T$
IIIF1SW-$P2^T$	pHC60 + *gfp*-tagged IIIF1SW-$P2^T$
IPTG	Isopropyl β-D-thiogalactoside
ISS	International Space Station
K_{cat}	Turnover number
K_m	Michaelis constant
Kp_*ansA*	Gene encoding cytoplasmic L-asparaginase I of IIIF1SW-$P2^T$
Kp_AnsA	Recombinant L-asparaginase I of *P. piersonii* IIIF1SW-$P2^T$
LB	Luria Bertani
L4	Fourth larval stage
LRT	Log-rank (Mantel-Cox) test
MEGA	Molecular evolutionary genetics analysis
MTT	3-(4,5-Dimethylthiazol-2-yl)-2,5-diphenyl-2H-tetrazolium bromide
NCBI	National centre for biotechnology information
NGM	Nematode growth medium
Ni–NTA	Nickel-nitrilotriacetic acid
OP50	*E. coli* OP50
PAO1	*Pseudomonas aeruginosa* PAO1
PBS	Phosphate buffered saline
PCR	Polymerase chain reaction
pET28a	Protein overexpression vector pET28a(+)
pHC60	*gfp* Expression vector pHC60
pET28a_Kp_*ansA*	pET28a(+) vector carrying L-asparaginase gene of IIIF1SW-$P2^T$
QMEAN	Qualitative model energy analysis
RAST	Rapid Annotation using subsystem technology
SDS-PAGE	Sodium dodecyl sulfate polyacrylamide gel electrophoresis
TA_Kp_*ansA*	TA cloning vector carrying L-asparaginase gene of IIIF1SW-$P2^T$
V_{max}	Maximum velocity
YU22	*P. piersonii* YU22

Pantoea piersonii IIIF1SW-$P2^T$ (basionym *Kalamiella piersonii* IIIF1SW-$P2^T$) is a multidrug-resistant bacterial species affiliated with the family *Erwiniaceae*, isolated and characterized from the Port panel of the Cupola, an observation deck for the crew inhabiting at the International Space Station (ISS)[1]. The present taxon was predicted to be a non-pathogen to humans based on the PathogenFinder[1]. However, *P. piersonii* YU22, a closely related strain that was isolated and described from the urine sample originating from a kidney stone patient in India, was found to stimulate struvite crystallization and exert cytotoxicity to the Human Embryonic Kidney 293 cell line (HEK 293 T) *in vitro*[2]. A series of subsequent reports indicated the widespread occurrence of the present taxon, including human saliva[3], blood[4,5], and tissue[6]. *Kalamiella piersonii* IIIF1SW-$P2^T$ was reclassified as *Pantoea piersonii* IIIF1SW-$P2^T$ based on phylogenomic analysis[7]. Detailed molecular studies may shed more light on the complex ecology and help us understand the persistence and prevalence of the present taxon at contrasting niches across the globe and Space.

L-asparaginase is an enzyme involved in the catalytic conversion of L-asparagine into aspartic acid and NH_4^+. Asparaginase has been isolated and characterized from various bacteria, such as *Stenotrophomonas maltophilia* EMCC2297[8], *Salmonella paratyphi*[9], *Burkholderia pseudomallei*[10], as well as from other resources[11,12]. The enzyme is also marketed as an antineoplastic drug since it constrains amino acid supply to tumour cells and blocks cell proliferation by interrupting asparagine-dependent protein synthesis[13]. Asparaginase has been tested extensively for its anticancer efficacy in general and acute lymphoblastic leukaemia in particular[8–12]. Recently, asparagine-driven NH_4^+ formation was identified and attributed to struvite crystallization by YU22[2,14]. However, the mechanistic insights of cytotoxicity and the preferred niche for colonization remain poorly understood.

The human urine association, asparagine-driven NH_4^+ formation and direct involvement in struvite crystallization identified in YU22, which shared the highest genomic relatedness (99%) with IIIF1SW-$P2^T$, prompted the present research. We hypothesized L-asparaginase-driven cytotoxicity and the ability of IIIF1SW-$P2^T$ to colonize the reproductive tract of a eukaryote and tested the hypothesis using HEK 293 T and *Caenorhabditis elegans* as *in vitro* and *in vivo* models, respectively.

Materials and methods

Bacteria and culture conditions

Pantoea piersonii IIIF1SW-P2^T (= DSM 108198 ^{T}) was procured from Leibniz-Institut DSMZ, Braunschweig. Cells were grown in nutrient agar (HiMedia, India) at 37 °C for 24–48 h. Competent cells of *Escherichia coli* DH5α and *E. coli* BL21 (DE3) were procured from Yeastern Biotech. Transformed DH5α and BL21 (DE3) were grown on Luria Bertani (LB) agar plates or liquid broth supplemented with ampicillin (50 µg ml^{-1}) and kanamycin (30 µg ml^{-1}) at 37 °C for 24 h. TA cloning vector, pET28a(+) overexpression vector and *gfp*-bearing pHC60 were procured from Yeastern Biotech, Novagen and NovoPro, respectively, and maintained in DH5α.

Engineering recombinant L-asparaginase overexpression system

Genomic DNA (gDNA) of IIIF1SW-P2^T was isolated and purified using a DNA isolation kit (MolBio). The full-length gene (1014 bp) encoding L-asparaginase (Kp_*ansA*) was amplified from gDNA of IIIF1SW-P2^T using NdeI restriction site-tagged forward (Kp_*ansA*_F: 5'-ATACATATGCAAAAGAAAAATATCTATG-3') and XhoI restriction site-tagged reverse primer (Kp_*ansA*_R: 5'-GTGCTCGAGTTAGTCTTCGGTCAGTTCA-3'), respectively. The PCR conditions were as follows: an initial denaturation at 95 °C for 2 min, and 35 cycles of denaturation at 95 °C for 30 s, annealing at 57 °C for 30 s and extension at 72 °C for 1.5 min followed by a final extension at 72 °C for 7 min. The NdeI/XhoI tagged amplicon was cloned to the TA cloning vector (Yeastern Biotech) using the manufacturer's protocol and the ligated product TA_Kp_*ansA* was introduced to DH5α through the heat shock method.

The positive transformants bearing TA_Kp_*ansA* appeared on ampicillin (25 µg/ml) supplemented LB agar were confirmed through colony PCR using M13F (5'-GTTTTCCCAGTCACGAC-3') and M13R (5'-TTCACAC AGGAAACAGCTATGAC-3') primers. The PCR conditions used for the amplification were as follows: an initial denaturation at 95 °C for 2 min, and 35 cycles of denaturation at 95 °C for 30 s, annealing at 55 °C for 30 s and extension at 72 °C for 1.5 min, followed by a final extension at 72 °C for 7 min. The amplicon was sequenced to verify the orientation and base pair errors using M13 primers. The TA_Kp_*ansA* construct was isolated from the transformants using the NucleoSpin plasmid extraction kit (Takara) and subjected to restriction double digestion using NdeI and XhoI enzymes (New England Biolabs) as per the manufacturer's protocol. The double digestion was verified through the agarose gel and the NdeI/XhoI-tagged gene was purified using NucleoSpin gel and PCR clean-up kit (Takara).

Simultaneously, pET28a(+) plasmid maintained at DH5α was extracted using NucleoSpin plasmid extraction kit (Takara) and subjected to NdeI/XhoI double digestion as per the manufacturer's protocol. Linearized plasmid was extracted from agarose gel using NucleoSpin gel and PCR clean-up kit (Takara). A 1014 bp amplicon was ligated to linearized pET28a(+) using T4 DNA ligase (New England Biolabs) as per the manufacturer's protocol. The pET28a(+)_Kp_*ansA* construct was introduced to competent BL21 (DE3) (Yeastern Biotech Co. Ltd) cells through heat shock transformation. Colony PCR was carried out to identify positive transformants using T7F (5'-TAATAGCACTCACTATAGGG-3') and T7R (5'-GCTAGTTATTGCTCAGCGG-3') primers. The PCR conditions were as follows: an initial denaturation at 95 °C for 2 min, and 35 cycles of denaturation at 95 °C for 30 s, annealing at 60 °C for 30 s and extension at 72 °C for 1.5 min followed by a final extension at 72 °C for 7 min.

Expression and purification of N-terminal His-tagged L-asaparaginase of IIIF1SW-P2^T

E. coli BL21 (DE3) cells transformed with pET28a(+)_Kp_*ansA* were cultivated in kanamycin (30 µg/ml) supplemented LB broth at 37 °C and 120 rpm till attainment of OD600 0.5. Expression of protein was induced by 1 mM (final concentration) isopropyl β-D-thiogalactoside (IPTG, HighMedia) and cells were cultured for an additional 4 h. The culture was centrifuged (10,000 rpm, 10 min, 4 °C) and pellets were suspended in 2 ml sodium phosphate buffer containing 10 mM imidazole. The cells were disrupted by sonication (5 s pulse, 20 s rest over 30 min) and centrifuged (12,000 rpm, 4 °C, 20 min). Recombinant L-asparaginase of *P. piersonii* IIIF1SW-P2^T (Kp_AnsA) was purified from supernatant using a Ni–NTA column chromatography with sodium phosphate buffer containing gradients of imidazole (20, 50, 100, 150, 200 and 250 mM) followed by dialysis (10 kDa cut-off).

Sodium dodecyl sulfate polyacrylamide gel electrophoresis and bradford assay

The purity and molecular mass of Kp_AnsA were assessed using Sodium Dodecyl Sulfate Polyacrylamide Gel Electrophoresis (SDS-PAGE). Denatured proteins were analyzed alongside a pre-stained protein ladder as a molecular mass reference. The target protein's theoretical molecular mass, derived from its amino acid sequence in SwissProt, was 37.975 kDa. For SDS-PAGE, 15 µl of each eluate was mixed with 5 µl of loading buffer and denatured at 95 °C for 5 min. The samples were resolved on a gel comprising a 5% acrylamide stacking gel (0.5 M Tris–Cl, pH 6.8) and a 10% acrylamide resolving gel (1.5 M Tris–Cl, pH 8.8) using a Bio-Rad system, with electrophoresis conducted over 75 min. The gel was stained with Coomassie Brilliant Blue for 60 min on an orbital shaker, followed by destaining with methanol:water:acetic acid (5:4:1, v/v) solution.

The protein concentration of the samples was determined through the Bradford method[15] using bovine serum albumin as a standard. The reaction mixtures were transferred to a 96-well microplate, and absorbance was measured at 595 nm using a microplate reader Asys UVM 340 (Biochrom, Holliston, MA, USA).

In silico prediction and molecular docking analysis

The theoretical isoelectric pH (pI) and molecular weight of the recombinant protein were predicted through pI and Mw tools of Expasy (https://web.expasy.org/compute_pi/). The domain search was carried out at UniProt using RKJ90748.1 as a query sequence. The 3D structure of L-asparaginase was predicted using Swiss-Model Software (http://swissmodel.expasy.org/), and the resulting models were further validated with ITASSER[16]. The Qualitative Model Energy Analysis (QMEAN) score and Ramachandran plot were used to analyse the quality

of the predicted model. Protein structures were prepared using the UCSF chimera protein preparation wizard (version 1.10). The 2D structures of the selected ligands were sourced from the PubChem database (https://pubchem.ncbi.nlm.nih.gov/). To explore the molecular interactions between the L-asparagine/glutamine and L-asparaginase, molecular docking using PyRx version 0.9.8[17] was performed with the default setting and the output files were analysed using Discovery Studio 2020 Client and Chimera version 1.10.

L-asparaginase assay

L-asparagine monohydrate was used as a substrate for the L-asparaginase assay. The NH_4^+ released was measured according to the method published elsewhere[18] with the microplate-scale modification of the experimental protocol[2]. Briefly, 95 µl of 1 mM L-asparagine prepared in phosphate buffer of pH 7 was mixed with 5 µl of purified enzyme. The reaction mixture was incubated at 37°C for 30 min and the reaction was terminated by the addition of 80 µl of sodium cocktail and sodium hypochlorite solution[18]. The plates were incubated for an additional 30 min to attain a stable color and read at 650 nm. The emerald green or blue coloration indicated the liberation of NH_4^+ and the amount of liberated NH_4^+ was calculated using a standard curve prepared for $(NH_4)_2SO_4$[2,18].

Effect of pH, temperature, metal ions and substrate concentrations on L-asparaginase

The optimum pH was determined by carrying out the enzymatic reaction in the buffer with a pH range of 4–9 (1 pH unit intervals). The optimum temperature for the catalytic activity was determined by maintaining the enzymatic reactions at 4, 25, 37, 50, 75 and 100°C. The effect of metal ions such as manganese, cobalt, potassium, magnesium, sodium, zinc, calcium and mercury was studied by incubating the enzyme with chloride salts of respective metal ions (20 mM). Relative activity of Kp_AnsA at various pH, temperature and metal ions were determined by comparing its activity to respective controls maintained at pH 7, 37 °C and 20 mM NaCl, respectively. The effect of the substrate concentration was determined by carrying out reactions with increasing concentration of L-asparagine (0–5 mM). The Michaelis constant (K_m), maximum velocity (V_{max}) and turnover number (K_{cat}) were calculated using GraphPad Prism version 8.

Phylogenetic analysis

The genes encoding cytoplasmic L-asparaginase I of IIIF1SW-P2^T (Locus tag: D7S44_08820; Protein: RKJ90748.1) and YU22 (Locus tag: EKL29_18180 Protein: RTY55432.1) were retrieved from their corresponding whole genome shotgun sequence data available at NCBI (GCA_003612015.1 and GCA_003970755.1, respectively). Closest related sequences were retrieved from the NCBI database through the BLASTp search. Reference amino acid sequences corresponding to asparaginases were also retrieved from the in-house bacterial genome collections maintained at RAST for additional phylogenetic analysis. The NCBI and RAST originated sequences were aligned independently through Clustal_X[19] and analysed via MEGA 5 (Molecular Evolutionary Genetics Analysis, version 5.0[20]). The evolutionary history was inferred by using the Maximum Likelihood method based on the JTT matrix-based model[21.] The tree visualized tough MEGA with the highest log likelihood is shown. The percentage of trees in which the associated taxa clustered together is shown next to the branches. Initial tree(s) for the heuristic search were obtained by applying the Neighbor-Joining method to a matrix of pairwise distances estimated using a JTT model. The tree is drawn to scale, with branch lengths measured in the number of substitutions per site. All positions containing gaps and missing data were eliminated. Tree topology was evaluated by using bootstrap resampling based on 1,000 replications[22].

In vitro cytotoxicity assay

HEK 293 T cell line procured from the National Centre for Cell Science in Pune, India, was cultured in Dulbecco's Modified Eagle's Medium supplemented with 10% fetal bovine serum and 1% antibiotic–antimycotic solution. Post-confluence of 70%, cells were trypsinized, centrifuged, and resuspended in cell line media (CLM), then seeded into a 96-well plate (5000 cells/well). After a 24 h incubation at 37 °C with 5% CO_2, HEK 293 T cells were cultivated in CLM, CLM supplemented with 0.5% (w/v) L-asparagine (CLMA), CLMA containing Kp_AnsA (CLMA_Kp_AnsA), CLM containing Kp_AnsA (CLM_Kp_AnsA) and aqueous NH_4OH (CLM_NH_4OH). Following treatment, MTT reagent (1 mg/mL) was added to the wells, and the plate was incubated for 4 h. The formazan crystals were dissolved in dimethyl sulfoxide and the absorbance was measured at 570 nm using a multimode reader.

Live-dead cell staining and quantification of residual NH_4^+

Cytotoxicity in the above-mentioned treatments was also evaluated through fluorescence microscopy using acridine orange-ethidium bromide (AO-EB) staining. HEK 293 T cells were plated (20,000 cells/well) and incubated for 24 h, followed by treatment as described under cytotoxicity assay for an additional 24 h. Cells were washed, and stained with 2 µg/ml of AO-EB for 15 min, excess stain was washed off using 1X PBS, cells were overlaid with PBS and examined under ZOE™ fluorescent cell imager, using green and red channels to assess differential viability. Results were compared to the untreated control. The NH_4^+ in the media supplied was quantified according to earlier descriptions[2,18].

Engineering *gfp*-tagged *P. piersonii* IIIF1SW-P2^T

Competent IIIF1SW-P2^T cells were prepared using the calcium chloride method, transformed with pHC60 using heat shock and grown on an LB plate containing tetracycline (20 µg ml^{-1}) for 24–48 h. The *gfp* expression in IIIF1SW-P2^T cells was achieved by adding 1 mM IPTG to LB agar. The expression of *gfp* was visualized through epifluorescence microscopy (excitation 475 nm; emission 509 nm).

Synchronisation of *Caenorhabditis elegans*

The worms were synchronized as per the earlier description[23] and cultured in Nematode Growth Medium (NGM), with *E. coli* OP50 lawn at 21 °C until maturity as described earlier[24]. Worms were collected after reaching a dense population by pouring M9 buffer over the plate. The sample was centrifuged (1500 rpm, 25 °C, 1 min), the pellet was resuspended in sodium hypochlorite solution, and shaken for 3 min to remove contaminants and separate eggs from adults. After rinsing twice with M9 buffer, the eggs were incubated at 16 °C overnight to hatch, ensuring a uniform population of larvae for assays.

C. elegans survival assay

The synchronized eggs were incubated at 16 °C for 3 days. Once the nematodes reached the L4 stage, the synchronized individuals were washed with 1 ml of S-basal buffer three times until the supernatant became clear. Twenty L4 nematodes were transferred to a fresh NGM plate containing 1 mM IPTG, inoculated with *gfp*-tagged IIIF1SW-P2^T (IIIF1SW-P2^T_pHC60). The impacts of OP50 and *P. aeruginosa* PAO1 and wild type IIIF1SW-P2^T on *C. elegans* were analysed in parallel. Bacterial suspensions ($\sim 1 \times 10^8$ CFU per ml each) were plated separately on NGM for the preparation of respective bacterial lawns. Dead worms were counted at 0, 2, 22 and 46 h of incubation.

Tracing *gfp*-tagged *P. piersonii* IIIF1SW-P2^T at the reproductive tract of *C. elegans*

L4 stage *C. elegans* were maintained on the lawn of *gfp*-tagged IIIF1SW-P2^T grown on LB supplemented with 1 mM IPTG for 2 h. The nematodes were picked up and observed under a fluorescence microscope (excitation 475; emission 509) for localization of *gfp*-tagged IIIF1SW-P2^T *in vivo*.

Time course analysis of *P. piersonii* IIIF1SW-P2^T colonization

Synchronized L4 nematodes ($n = 20$) were transferred to an NGM plate containing 1 mM IPTG, inoculated with *gfp*-tagged IIIF1SW-P2^T (IIIF1SW-P2^T_pHC60), and incubated at 21 °C. Worms were collected 0.5, 2, 22, and 46 h post-exposure for fluorescence imaging analysis. The worms were placed on the glass slide and immobilized using 5% (v/v) aqueous methanol. After mounting the coverslip, the worms were observed using the ZOE™ fluorescent cell imager.

Sustained colonization and fluorescence measurement

Synchronized L4 nematodes ($n = 20$) were transferred to an NGM plate containing 1 mM IPTG, inoculated with *gfp*-tagged IIIF1SW-P2^T (IIIF1SW-P2^T_pHC60). Worms were also simultaneously transferred to separate NGM plates containing wild-type IIIF1SW-P2^T, OP50 and PAO1 in parallel. Worms were collected at 0.5, 2, 22, and 46 h post-exposure for fluorescence imaging analysis. The worms were placed on the glass slide and immobilized using 5% (v/v) aqueous methanol. After mounting the coverslip, the worms were observed using ZOE™ fluorescent cell imager. The vulvar region of *C. elegans* was examined for sustained colonization. Fluorescence images of *C. elegans* expressing *gfp* were analysed using ImageJ software. A fixed region of interest covering only the vulvar region, measuring an area of 2500 pixels^2 was manually selected to measure total fluorescence. The integrated density was used to estimate the fluorescence intensity.

Statistical analysis

Statistical significance was determined by either ordinary one-way analysis of variance (ANOVA) with Tukey's multiple comparisons test or *t*-test using GraphPad Prism ($^*P < 0.1$, $^{**}P < 0.05$, $^{***}P < 0.01$, $^{****}P < 0.0001$; ns, non-significant), unless specified otherwise.

Results

Molecular and phylogenetic characterization of L-asparaginase of IIIF1SW-P2^T

The gene encoding cytoplasmic L-asparaginase I (Kp_*ansA*, 1014 bp; D7S44_08820) of IIIF1SW-P2^T shared absolute nucleotide sequence similarity with that of YU22 (EKL29_18180). The theoretical pI and molecular weight of the L-asparaginase I of IIIF1SW-P2^T were estimated to be 5.84 and 36,954.94 Da, respectively. Ni–NTA purified recombinant L-asparaginase of IIIF1SW-P2^T (Kp_AnsA) complied with the theoretical molecular weight as evident through SDS PAGE analysis (Fig. 1a, Supplementary Fig. S1). The domain search at UniProt revealed the asparaginase domain (position 5–188) at the N-terminus and glutaminase domain (position 213–326) at the C-terminus. The QMEN score of the L-asparaginase model was 0.04, while the Global Model Quality Estimation score was 0.90. The Ramachandran plot analysis showed that 95.58% of the residues were within the allowed region. Binding energy scores of −6.0 kcal/mol and −5.5 kCal/mol, respectively, were obtained for Kp_AnsA while using L-asparagine and glutamine as ligands during the docking study. L-asparagine predicted to establish hydrogen bond with Thr14, Ser 60, Ser61, Thr91, Asp92, Lys163 and Asn246 of Kp_AnsA (Fig. 1b–c). In contrast, glutamine established hydrogen bonds with Thr14, Thr91, Asp92, Ser117, Gln118 and Lys163. These two ligands also varied in terms of residues that established Van der Waals forces of attraction. These data suggested the possible involvement of Thr14, Thr91, Asp92 and Lys163 as common catalytic site residues for L-asparagine and glutamine.

Enzyme assays were carried out for Kp_AnsA using L-asparagine as a substrate. Michaelis constant (K_m) was found to be 5.4 mM for Kp_AnsA. Enzymatic analysis revealed a maximum velocity (V_{max}) and turnover number (K_{cat}) of 8.4 U/mg and 135.6 µmoles s^{-1}, respectively (Fig. 1d). The enzyme was found to be highly active in pH 8–10 (optimum pH 9) and 37 °C (Fig. 1e–f, respectively). The enzyme exhibited statistically similar activity when provided with diverse metal ions, except for cobalt and mercury that suppressed the catalysis (Fig. 1g). Kp_AnsA formed a tight (83% bootstrap confidence of the node) coherent cluster with that of strains of *P. piersonii* during maximum likelihood phylogenetic analysis (Fig. 1h). The analysis using randomly chosen genome-sequenced

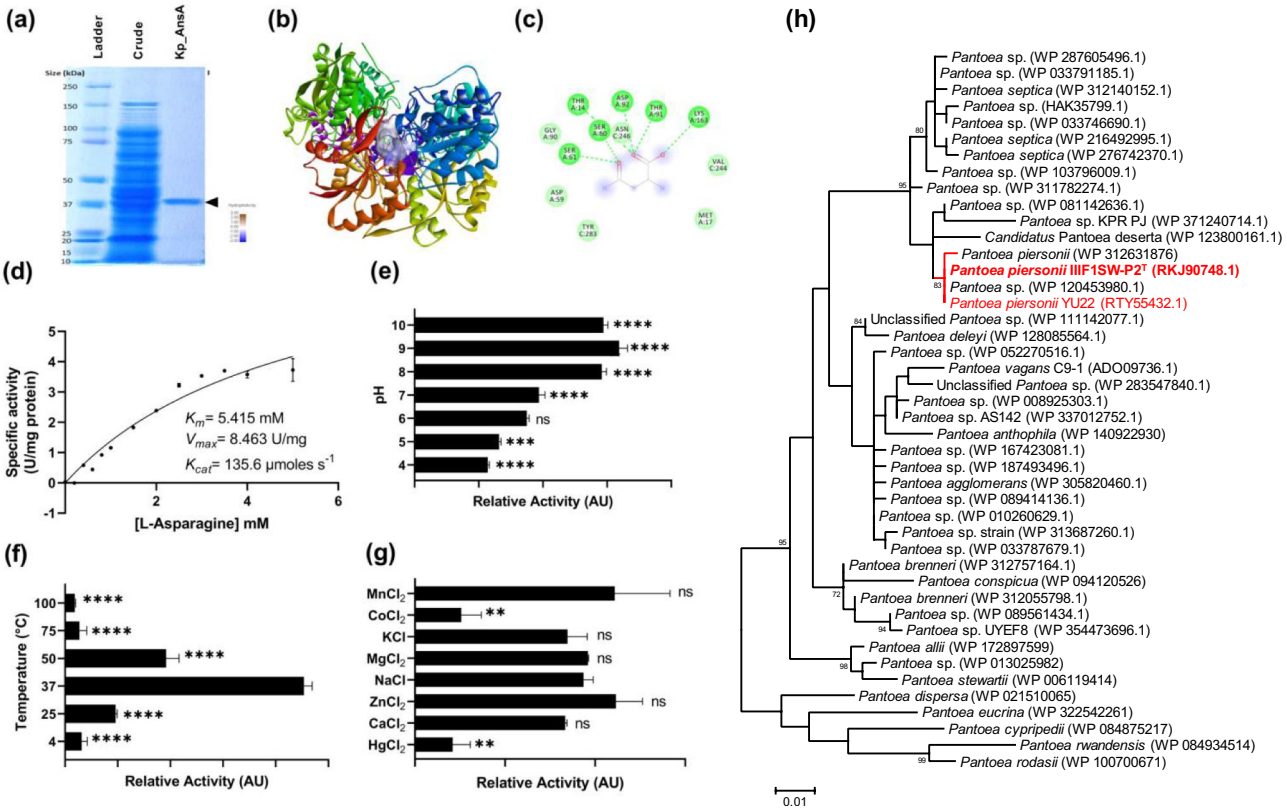

Fig. 1. Purification, characterization and phylogenetic analysis of recombinant L-asparaginase from *Pantoea piersonii* IIIF1SW-P2^T (Kp_AnsA), overexpressed in *Escherichia coli* BL21 (DE3). SDS PAGE analysis of Ni–NTA affinity chromatography purified Kp_AnsA (**a**, arrowhead), its substrate (Asparagine) binding site (**b**), active site residues (**c**), enzyme kinetics (**d**), influence of pH (**e**), temperature (**f**) and metal ions (**g**) are shown. Additional details of SDS PAGE can be found in Fig. S1. Reactions maintained at pH 7, 37 °C and NaCl were used as controls for pH (**e**), temperature (**f**) and metal ion (**g**) assays, respectively. Error bar, mean (n = 2) ± SD. Statistical significance was determined through ordinary One-way ANOVA (Dunnett's multiple comparison test). $^*P < 0.1$, $^{**}P < 0.05$, $^{***}P < 0.01$, $^{****}P < 0.0001$; ns, non-significant. Unrooted maximum likelihood tree of amino acid sequences depicting the phyletic lineage of *P. piersonii* IIIF1SW-P2^T and other bacterial species/strains of closest sequence match (h). Bootstrap values of > 70% after 1,000 bootstrap replicates are shown at the branch points. Reference sequences were retrieved from NCBI. Bar, 0.01 substitutions per site.

bacterial species revealed a tight (99% bootstrap confidence of the node) phylogenetic neighborhood formed between Kp_AnsA and *Idiomarina tyrosinivorans* CC-PW-9 ^{T}, a marine bacterial species (Fig. S2). Several new bacterial species isolated from marine samples were also formed a tight adjacent clade. Thus, both IIIF1SW-P2^T and YU22 found to produce structurally identical L-asparaginase, which is active at 37 °C, pH 8–10 and in the presence of diverse metal ions.

L-asparaginase-mediated NH_4^+ generation is cytotoxic to HEK 293 T

The possible cytotoxicity of bacterial L-asparaginase on HEK 293 T was investigated. The impacts of pure Kp_AnsA (1.5 µg per well; final concentration) on HEK 293 T were tested in the presence/absence of 0.5% (w/v) L-asparagine as a substrate. The extent of cytotoxicity exerted by Kp_AnsA on HEK 293 T was assessed qualitatively and quantitatively using AO/EB staining. Fluorescence microscopy showed enhanced cytotoxicity in HEK 293 T cells in the presence of Kp_AnsA and L-asparagine (CLMA_Kp_AnsA) as compared to that of enzyme-free L-asparagine-amended media (CLMA) (Fig. 2a). Similarly, cytotoxicity was also found when HEK 293 T cells were treated with enzyme without L-asparagine (CLM_Kp_AnsA). HEK 293 T cells treated with standard NH_4OH (CLM_NH_4OH) also displayed cytotoxicity. Kp_AnsA enhanced cytotoxicity was substantiated through fluorescent measurements where significantly ($P < 0.0001$) high fluorescence was detected emitting from cells treated with CLMA_Kp_AnsA as compared to that of CLMA (Fig. 2b). Similarly, significant fluorescent intensity was detected in HEK 293 T cells when exposed to L-asparagine-free media (CLM_Kp_AnsA), suggesting L-asparagine-independent NH_4^+ formation. Fluorescence response of HEK 293 T cells treated exclusively with standard NH_4OH (CLM_NH_4OH) validated NH_4^+ driven cytotoxicity. Thus, fluorescence microscopy provided preliminary evidence for the susceptibility of HEK 293 T to NH_4^+, a by-product of enzymatic degradation of L-asparagine.

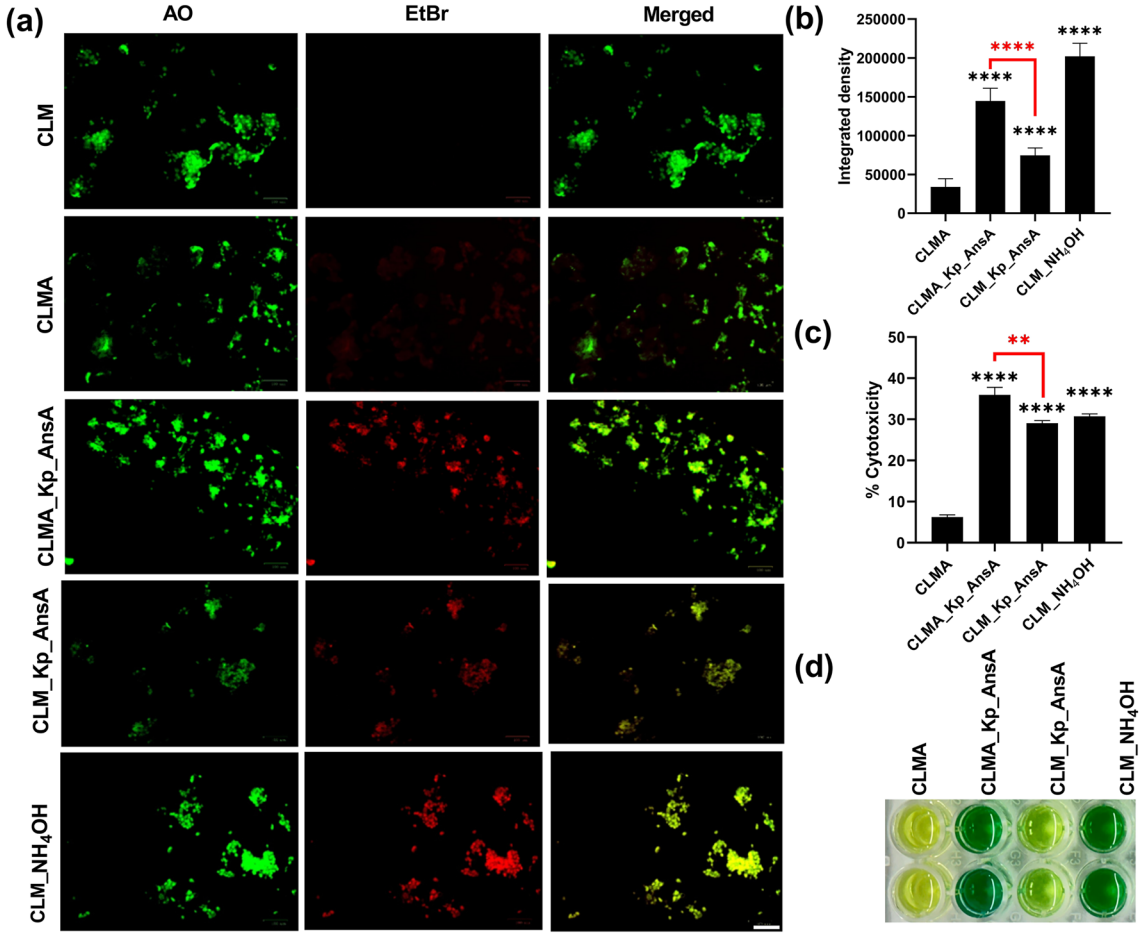

Fig. 2. Cytotoxic impacts of purified recombinant L-asparaginase of *Pantoea piersonii* IIIF1SW-P2^T (Kp_AnsA) on Human Embryonic Kidney 293 (HEK 293 T) cells (**a**-**c**) and chromogenic reactions showing differential NH_4^+ content (**d**). The response of HEK 293 T cells cultivated in cell line media (CLM), CLM supplemented with 0.5% asparagine (CLMA), CLMA containing Kp_AnsA (CLMA_Kp_AnsA), CLM containing Kp_AnsA (CLM_Kp_AnsA) and aqueous NH_4OH (CLM_NH_4OH) after live/dead assay done through acridine orange-ethidium bromide (a) and corresponding CLM-subtracted fluorescent intensity of merged image (b) are shown. Cytotoxicity (%) of HEK 293 T in CLMA, CLMA_Kp_AnsA, CLM_Kp_AnsA and CLM_NH_4OH are shown (b). Chromogenic reactions displaying the differential presence of NH_4^+ in CLMA, CLMA_Kp_AnsA, CLM_Kp_AnsA and CLM_NH_4OH are shown (b). CLMA was used as a control in (b) and (c) for statistical analysis. Error bar in (b), mean (n = 7) ± SD; Error bar in (c), mean (n = 3) ± SD; ****$P < 0.0001$; **$P < 0.01$. Red asterisks display a significant level based on *t*-test.

Kp_AnsA-driven cytotoxicity on HEK 293 T was assessed further using the MTT assay. Significant ($P < 0.0001$) cytotoxicity was detected in cells treated with CLMA_Kp_AnsA as compared to that of CLMA (Fig. 2c). Significant ($P < 0.0001$) cytotoxicity was also detected in HEK 293 T cells when treated with L-asparagine-free media (CLM_Kp_AnsA), substantiating L-asparagine-independent NH_4^+ formation. HEK 293 T cells treated with standard NH_4OH (CLM_NH_4OH) displayed significant ($P < 0.0001$) cytotoxicity, further validating the direct involvement of NH_4^+. The colorimetric analysis showed high amounts of NH_4^+ in asparaginase amended CLMA containing Kp_AnsA (CLMA_Kp_AnsA, 15.5 µM, $P < 0.0001$), followed by CLM_NH_4OH (12.7 µM, $P < 0.0001$) and CLM_Kp_AnsA (4.1 µM, $P < 0.0001$) as compared to CLMA (Fig. 2d). These findings were in line with that of the live-dead staining assay, wherein L-asparagine-amended media in the presence of L-asparaginase and media with aqueous NH_4OH induced cell death in HEK 293 T cells, as indicated by the presence of yellow fluorescing nuclei in the merge channel images.

Rapid and sustained colonization of IIIF1SW-P2^T at the reproductive tract of *C. elegans*

The potential ability of IIIF1SW-P2T to colonize the eukaryotic reproductive tract *in vivo* was investigated using *C. elegans* as a model system. The worms were introduced to NGM plates containing a lawn of *gfp*-tagged cells of IIIF1SW-P2^T and monitored under fluorescence microscopy. We found distinct colonization of IIIF1SW-P2^T at the vulvar and adjacent luminal region of *C. elegans* (Fig. 3a-b). The intense fluorescence corresponding to IIIF1SW-P2^T cells was not evident at the mouth and anal region of the *C. elegans*, suggesting that IIIF1SW-P2^T cells specifically colonize the reproductive tract of the nematode. The colonization of the reproductive tract was

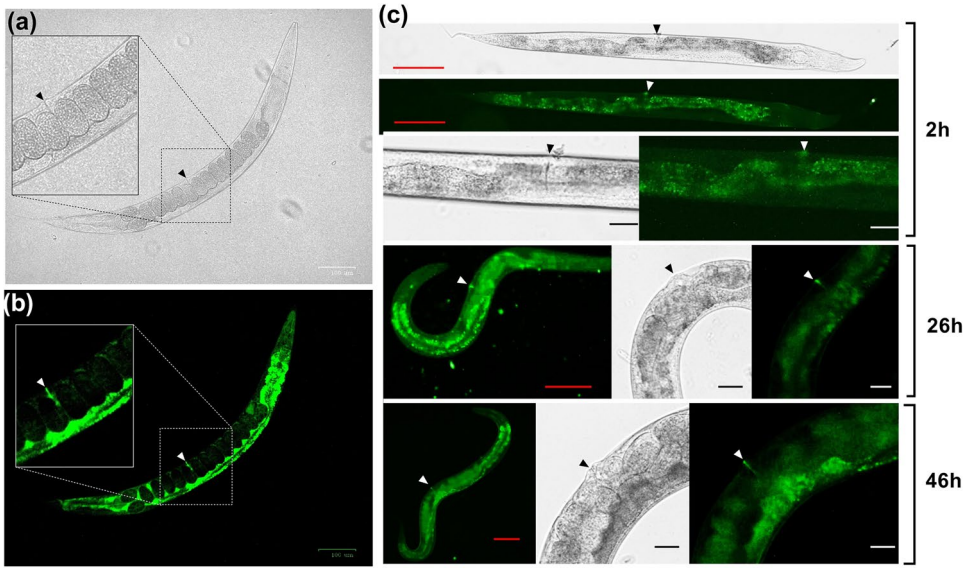

Fig. 3. Localization and time course of colonization of *gfp*-tagged *Pantoea piersonii* IIIF1SW-P2^T (IIIF1SW-P2^T_pHC60) at the reproductive tract of *Caenorhabditis elegans*. Bright field (**a**) and fluorescent (**b**) microscopic images showing the colonization of IIIF1SW-P2^T_pHC60 at the anterior reproductive tract of *C. elegans*. Scale bar, 100 µm. Bright-field and fluorescence micrographs showing the time course of colonization of IIIF1SW-P2^T_pHC60 in the reproductive tract of hermaphrodite *C. elegans* as evident after 2 h, 26 h and 46 h of infection (**c**). Arrowhead shows colonization at the vulvar and luminal regions. Red scale bar, 100 µm; black/white scale bar, 25 µm.

found to initiate as early as 2 h of grazing and was found consistent till the completion (46 h) of the experiments (Fig. 3c). The time course analysis revealed rapid, sustained and specific luminal colonization of IIIF1SW-P2^T_pHC60 at the reproductive tract of *C. elegans*.

The impacts of IIIF1SW-P2^T on the survival of *C. elegans* was assessed. Synchronized worms were left to graze on the plates containing wild-type IIIF1SW-P2^T, IIIF1SW-P2^T_pHC60, OP50 and PAO1. *C. elegans* treated with wild-type IIIF1SW-P2^T and IIIF1SW-P2^T_pHC60 were highly motile due to enhanced undulatory movements as compared to the worms treated with OP50. IIIF1SW-P2^T (with and without *gfp*-tagging) exhibited marginal killing capacity, with higher mean lifespan and survival over time when compared to PAO1 (LRT: P = 0.0079; GBWT: P = 0.0097) and slightly decreased mean lifespan and survival over time when compared to OP50 (LRT: P = 0.0253; GBWT: P = 0.0253) (Fig. 4a). Fluorescence signals emitted from hermaphrodite worms were assessed after treating with IIIF1SW-P2^T, IIIF1SW-P2^T_pHC60, OP50 and PAO1. The low and high magnification bright field and fluorescence micrographs of *C. elegans* treated with IIIF1SW-P2^T (Fig. 4b), IIIF1SW-P2^T_pHC60 (Fig. 4c), OP50 (Fig. 4d) and PAO1 (Fig. 4e) consistently showed the autofluorescence of varying intensity emitting from the worm body. However, elevated gut fluorescence was observed in *C. elegans* treated with IIIF1SW-P2^T_pHC60. Extensive analysis of the vulvar region revealed fluorescence signals corresponding to IIIF1SW-P2^T_pHC60 emitting from the embryos and interembryonic space apart from the vulvar/luminal regions (Fig. 4c). In contrast, such signals were absent in the worms treated with OP50 and PAO1. Integrated density measurement revealed significantly high fluorescence emitting from IIIF1SW-P2^T_pHC60 followed by IIIF1SW-P2^T (Fig. 4f). In contrast, weak fluorescence signals were detected in the vulvar regions of worms treated with OP50 and PAO1. These data indicated the potential ability of IIIF1SW-P2^T to colonize the reproductive tract of *C. elegans* with mild lethality to the host.

Discussion

Bacterial L-asparaginases have been well studied for their cytotoxicity, particularly on cancer cells[8–10,12,13]. The constraint in the bioavailability of L-asparagine driven by L-asparaginase, as the latter readily converts L-asparagine to aspartic acid, is regarded as one of the mechanisms causing cancer cell death[13]. However, the role of NH_4^+, a by-product of the catalytic breakdown of L-asparagine, in cytotoxicity remained unexplored. The rapid formation of NH_4^+ and significant upregulation of the asparaginase gene in YU22 when exposed to L-asparagine[2,14] prompted this investigation on the ISS counterpart. Asparaginase-driven NH_4^+ formation was demonstrated to trigger struvite crystallization in urease-negative YU22[2]. A subsequent study showed an alternative ATP-dependent catabolic pathway driven by urea carboxylase and allophanate hydrolase acting upon urea, possibly contributing to NH_4^+ formation[14]. Asparaginase-driven NH_4^+ formation, which is an ATP-independent process, appears to be one of the important virulence factors that provides a competitive advantage to the pathogen to thrive under extreme conditions of the reproductive tract. The amino acids and small peptides present in the urine serve as carbon sources for the bacteria residing in the urinary tract[25,26]. Asparagine is identified as one of the lifespan-decreasing amino acids for *C. elegans*[27]. The enzyme kinetics data presented here

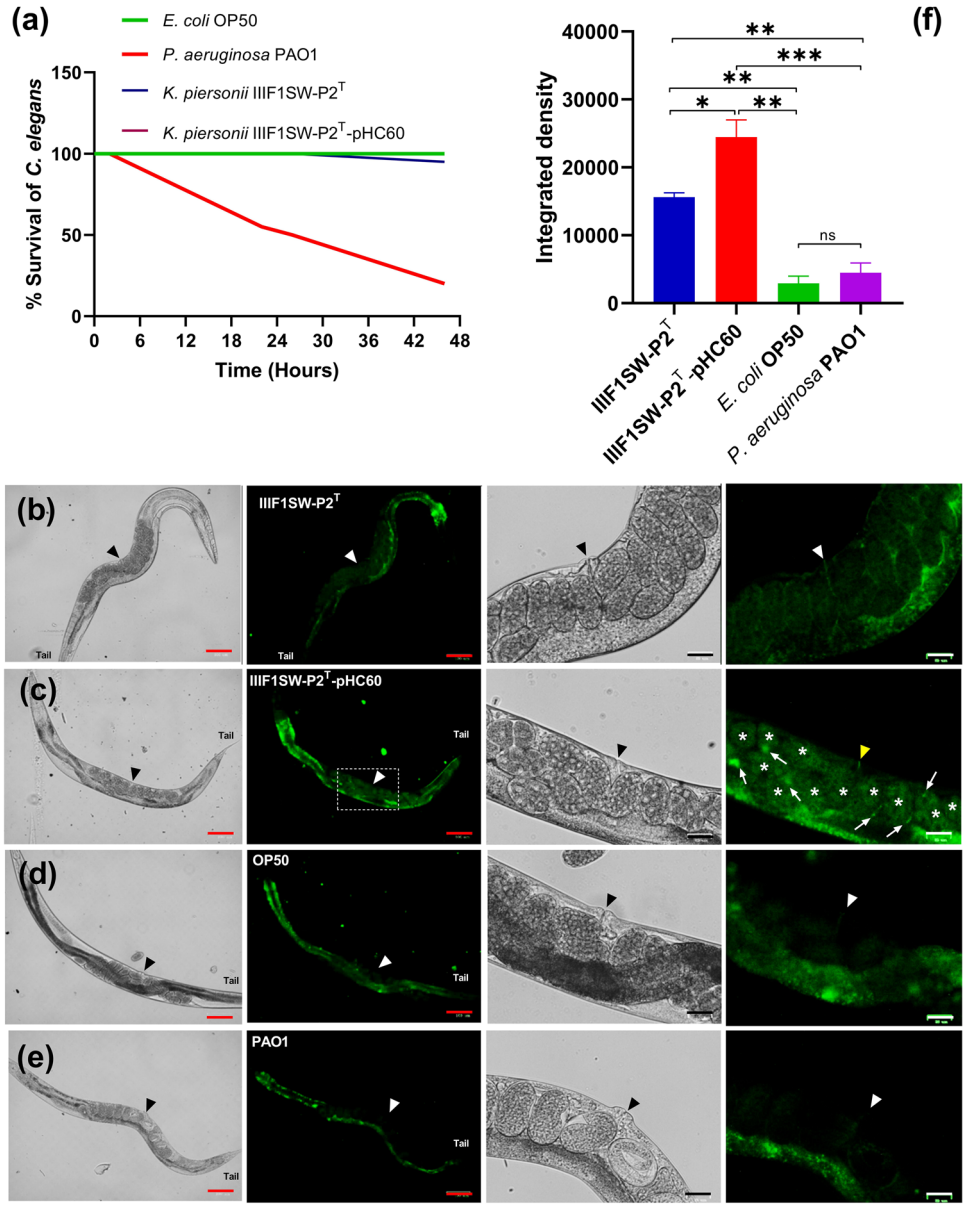

Fig. 4. Survival assay and demonstration of sustained colonization of *P. piersonii* IIIF1SW-P2^T at the reproductive tract. Percent survival was averaged across experimental replicates, before the calculation of differences in mean lifespan and survival over time of *gfp*-tagged *P. piersonii* IIIF1SW-P2^T (*P. piersonii* IIIF1SW-P2^T_pHC60) compared to wild-type *P. piersonii* IIIF1SW-P2^T, *P. aeruginosa* PAO1 (positive control) and *E. coli* OP50 (negative control). Statistical significance was measured through the Log-rank (Mantel-Cox) test and the Gehan-Breslow-Wilcoxon test. Low and high magnification bright field and fluorescence micrographs showing bacterial colonization in hermaphrodite *C. elegans* (b). The bright field and fluorescence responses of *C. elegans* treated with wild-type *P. piersonii* IIIF1SW-P2^T (**a**), *gfp*-tagged *P. piersonii* IIIF1SW-P2^T (IIIF1SW-P2^T_pHC60) (**b**), OP50 (**c**) and PAO1 (**d**) are shown. The expression of *gfp* in (b) was achieved using 1 mM IPTG. The vulvar region is highlighted in a black/white arrowhead. Colonization in the vulvar region, including the lumen, embryos and extraembryonic space, are highlighted through yellow arrowhead, white asterisks and white arrow, respectively. Red scale bar, 100 µm; black/white scale bars 25 µm. (**e**), fluorescent intensity detected in *C. elegans* across various treatments. Statistical comparisons were made using one-way ANOVA followed by Tukey's multiple comparisons test. Error bar, mean (n = 4) ± SD. $^*P < 0.1$, $^{**}P < 0.05$, $^{***}P < 0.01$, $^{****}P < 0.0001$; ns, non-significant.

validated the active enzymatic formation of NH_4^+ from a simple amino acid L-asparagine. While NCBI-based phylogenetic analyses confirmed the proximity of purified enzyme to *Pantoea*, RAST-based analysis revealed its similarity to that of bacterial isolates of marine origins, substantiating the halotolerance.

An earlier study has employed the HEK 293 T cell line to demonstrate the adhesion and cytotoxicity of YU22[2]. In this study, the impacts of purified recombinant Kp_AnsA on HEK 293 T cell line were investigated to decode the

mechanism of cytotoxicity. NH_4^+ generated through the catalytic activity of Kp_AnsA on L-asparagine resulted in cytotoxicity. In contrast, cytotoxicity observed in the absence of L-asparagine is most likely due to the activity of Kp_AnsA on an alternative substrate, possibly glutamine present in the cell culture media. Our analysis *in silico* predicted the glutaminase domain in the C-terminus of Kp_AnsA. However, further studies are warranted to validate Kp_AnsA-driven NH_4^+ formation from alternative substrates. Mild toxicity detected in enzyme-free L-asparagine amended media (CLMA) is most likely due to the residual NH_4^+ impurities originating from L-asparagine/or spontaneous degradation of L-asparagine. The assessment of possible aspartate-driven toxicity was not possible in the current experimental setup. Furthermore, the enzyme and substrate concentrations during *in vitro* study were optimized to get detectable signals in colorimetric and fluorimetric analyses. The physiological and pathophysiological relevance of the tested doses of enzyme, substrate and product warrants further investigation using *in vivo* model.

C. elegans shares key genetic and physiological similarities with humans and hence being used as one of the potential non-mammalian model organisms to investigate ageing and the onset, progression and pathophysiology of various human disorders, including Alzheimer's and Parkinson's diseases[28–30]. Hermaphrodite *C. elegans* shares some reproductive similarities with human females and hence is proposed as a powerful high-throughput model to study the female reproductive health[31]. In this study, green fluorescence was consistently observed in the *C. elegans* gut irrespective of the bacterial treatment. This is probably due to intestinal autofluorescence that arises due to fluorophores (age pigments) of gastrointestinal tract[32]. The autofluorescent molecules are spectrally heterogeneous with distinct biological properties, and can be used as a non-invasive biomarker to probe senescence and advanced glycation end products *in vivo*[30,32]. While red autofluorescence is a candidate marker for health as it correlates well with an individual's remaining days of life, blue autofluorescence is proposed to be an indicator of an individual's incipient or recent demise[32]. In contrast, green autofluorescence is an ill-suited probe either for life or death since it combines both properties and extreme caution needs to be taken to distinguish *gfp* expression near the time of death from full-body fluorescence[32]. In this study, live worms were taken for imaging after brief methanol treatment in order to probe the colonization of target organisms. The distinct emission of green fluorescence at the vulva, lumen, uterus, eggs and embryos substantiated the rapid and sustained colonization of IIIF1SW-P2^T at the reproductive tract. However, further studies are needed to discriminate the gut colonization of IIIF1SW-P2^T_pHC60 and the autofluorescence emitting from the gastrointestinal tract of *C. elegans*.

C. elegans is reported to be a facile and inexpensive model host for investigating several Gram-positive bacterial pathogens infecting humans[33]. The lethal impacts of *Enterococcus faecalis*, *Streptococcus pneumoniae*, and *Staphylococcus aureus*, but not *Bacillus subtilis*, *Enterococcus faecium*, or *Streptococcus pyogenes*, on *C. elegans* have been documented. Another study identified diminished capacity of aged *C. elegans* to control intestinal bacterial accumulation[34]. These two studies emphasized the differential compatibility of *C. elegans* to pathogenic bacteria and suggested the insufficiency of a single exposure to track colonisation. Although the bacteria are the essential nutritional source of *C. elegans*, some pathogenic bacteria may cause infection and death to the nematode[35]. For example, *Microbacterium nematophilum* was demonstrated to cause distinct modes of infection and host response since it adheres to the rectal and post-anal cuticle, mimicking the natural infection of *C. elegans*[36]. Therefore, monitoring the colonization and clearance dynamics alongside the survival was necessary[33,34]. Therefore, the time course of colonization of IIIF1SW-P2^T at the reproductive tract and survival of worms were invetigated in parallel. Our study revealed rapid and sustained colonization of IIIF1SW-P2^T at the reproductive tract of *C. elegans* with mild mortality to the host. *gfp*-tagged IIIF1SW-P2^T were localized in the vulvar area, including the vulvar lumen, which connects the vulva with the uterus required for mating and egg-laying[37]. In contrast, significant mortality observed after PAO1 treatment aligned with the previous reports on *Pseudomonas* representatives that impart lethality in *C. elegans*[38–41].

Conclusion

A recombinant L-asparaginase of IIIF1SW-P2^T (Kp_AnsA) was produced using *E. coli* BL21 (DE3), and its cytotoxic attributes on HEK 293 T cell line were demonstrated. Kp_AnsA was found to be a halotolerant enzyme phylogenetically related to asparaginases of marine bacteria and found to be highly active at alkaline pH. The recombinant Kp_AnsA with a molecular weight of 37.975 kDa displayed K_m, V_{max} and K_{cat} values of 5.4 mM, 8.4 U/mg and 135.6 µmoles s^{-1} versus L-asparagine and was found to readily generate NH_4^+ ions *in vitro*. The catalytic formation of NH_4^+ from L-asparagine underpins cytotoxicity in HEK 293 T. Assays *in vivo* using *gfp*-tagged cells revealed the rapid and sustained colonizing ability of IIIF1SW-P2^T at the vulva, luminal region, embryo and interembryonic space of *Caenorhabditis elegans,* with mild mortality on the host. Thus, *C. elegans* and IIIF1SW-P2^T appear to be a potential infection model to investigate reproductive health. The role played by L-asparaginase in the colonization of IIIF1SW-P2^T at the reproductive tract of *C. elegans* merits further investigation.

Data availability

The datasets used and/or analysed during the current study available from the corresponding authors Dr. Asif Hameed & Dr. Rajesh P. Shastry on reasonable request.

Received: 16 March 2025; Accepted: 8 September 2025
Published online: 09 October 2025

References

1. Singh, N. K., Wood, J. M., Mhatre, S. S. & Venkateswaran, K. Metagenome to phenome approach enables isolation and genomics characterization of *Kalamiella piersonii* gen. nov., sp. nov. from the International Space Station. *Appl Microbiol Biotechnol* **103**, 4483–4497. https://doi.org/10.1007/s00253-019-09813-z (2019).
2. Rekha, P. D. et al. First report of pathogenic bacterium *Kalamiella piersonii* isolated from urine of a kidney stone patient: draft genome and evidence for role in struvite crystallization. *Pathogens* https://doi.org/10.3390/pathogens9090711 (2020).
3. McDonagh, F. et al. First complete genome of a multidrug-resistant strain of the novel human pathogen *Kalamiella piersonii* (GABEKP28) identified in human saliva. *J Glob Antimicrob Resist* **32**, 31–34. https://doi.org/10.1016/j.jgar.2022.12.003 (2023).
4. Howard, M., Maki, J. J., Connelly, S., Hardy, D. J. & Cameron, A. Complete genome sequence of a human bacteremia isolate of *Kalamiella piersonii*. *Microb Resour Announc* **12**, e0029323. https://doi.org/10.1128/MRA.00293-23 (2023).
5. Sada, J. et al. Bacteremia caused by *Kalamiella piersonii* found in an infant during the course of gastrointestinal food allergy. *Infect Drug Resist* **16**, 2647–2651 (2023).
6. Atilan, K., Ozdem, T., Aydogan, C. N. & Hosbul, T. A rare case report of tissue infection caused by *Pantoea piersonii* (basionym *Kalamiella piersonii*). *Folia Microb (Praha)* https://doi.org/10.1007/s12223-024-01203-x (2024).
7. Soutar, C. D. & Stavrinides, J. Phylogenomic analysis of the *Erwiniaceae* supports reclassification of *Kalamiella piersonii* to *Pantoea piersonii* comb. nov. and *Erwinia gerundensis* to the new genus *Duffyella* gen. nov. as *Duffyella gerundensis* comb. nov. *Mol Genet Genomics* **297**, 213–225. https://doi.org/10.1007/s00438-021-01829-3 (2022).
8. Abdelrazek, N. A., Saleh, S. E., Raafat, M. M., Ali, A. E. & Aboulwafa, M. M. Production of highly cytotoxic and low immunogenic L-asparaginase from *Stenotrophomonas maltophilia* EMCC2297. *AMB Express* **14**, 51. https://doi.org/10.1186/s13568-024-01700-9 (2024).
9. Abdullah, E. M. et al. Expression, characterization and cytotoxicity of recombinant l-asparaginase II from *Salmonella paratyphi* cloned in *Escherichia coli*. *Int J Biol Macromol* **279**, 135458. https://doi.org/10.1016/j.ijbiomac.2024.135458 (2024).
10. Darwesh, D. B. et al. Anticancer activity of extremely effective recombinant L-asparaginase from *Burkholderia pseudomallei*. *J. Micro. Biotechnol.* **32**, 551–563. https://doi.org/10.4014/jmb.2112.12050 (2022).
11. Borges, G. A. et al. Asparaginase induces selective dose- and time-dependent cytotoxicity, apoptosis, and reduction of NFκB expression in oral cancer cells. *Clin. Exp. Pharmacol. Physiol.* **47**, 857–866. https://doi.org/10.1111/1440-1681.13256 (2020).
12. Serravalle, S., Bertuccio, S. N., Astolfi, A., Melchionda, F. & Pession, A. Synergistic Cytotoxic Effect of L-Asparaginase Combined with Decitabine as a Demethylating Agent in Pediatric T-ALL, with Specific Epigenetic Signature. *Biomed Res International* **2016**, 1985750. https://doi.org/10.1155/2016/1985750 (2016).
13. Narta, U. K., Kanwar, S. S. & Azmi, W. Pharmacological and clinical evaluation of L-asparaginase in the treatment of leukemia. *Crit Rev Oncol Hematol* **61**, 208–221. https://doi.org/10.1016/j.critrevonc.2006.07.009 (2007).
14. Yuvarajan, S., Hameed, A., Arun, A. B., Saptami, K. & Rekha, P. D. Urease-negative uropathogen *Kalamiella piersonii* YU22 metabolizes urea by urea carboxylase and allophanate hydrolase enzyme system. *Microb Res* **263**, 127142. https://doi.org/10.1016/j.micres.2022.127142 (2022).
15. Hammond, J. B. & Kruger, N. J. The bradford method for protein quantitation. *Methods Mol Biol* **3**, 25–32. https://doi.org/10.1385/0-89603-126-8:25 (1988).
16. Yang, J. Y. et al. The I-TASSER Suite: protein structure and function prediction. *Nat. Methods* **12**, 7–8. https://doi.org/10.1038/nmeth.3213 (2015).
17. Dallakyan, S. & Olson, A. J. Small-molecule library screening by docking with PyRx. *Methods Mol Biol* **1263**, 243–250. https://doi.org/10.1007/978-1-4939-2269-7_19 (2015).
18. Baethgen, W. E. & Alley, M. M. A manual colorimetric procedure for measuring ammonium nitrogen in soil and plant Kjeldahl digests Commun Soil Sci. *Plant Anal.* **20**(961), 969 (1989).
19. Thompson, J. D., Gibson, T. J., Plewniak, F., Jeanmougin, F. & Higgins, D. G. The CLUSTAL_X windows interface: flexible strategies for multiple sequence alignment aided by quality analysis tools. *Nucleic Acids Res* **25**, 4876–4882. https://doi.org/10.1093/nar/25.24.4876 (1997).
20. Tamura, K. et al. MEGA5: molecular evolutionary genetics analysis using maximum likelihood, evolutionary distance, and maximum parsimony methods. *Mol Biol Evol* **28**, 2731–2739. https://doi.org/10.1093/molbev/msr121 (2011).
21. Jones, D. T., Taylor, W. R. & Thornton, J. M. The rapid generation of mutation data matrices from protein sequences. *Comput Appl Biosci* **8**, 275–282. https://doi.org/10.1093/bioinformatics/8.3.275 (1992).
22. Felsenstein, J. Confidence limits on phylogenies: an approach using the bootstrap. *Evolution* **39**, 783–791. https://doi.org/10.1111/j.1558-5646.1985.tb00420.x (1985).
23. Bajire, S. K., Jain, S., Johnson, R. P. & Shastry, R. P. 6-Methylcoumarin attenuates quorum sensing and biofilm formation in *Pseudomonas aeruginosa* PAO1 and its applications on solid surface coatings with polyurethane. *Appl Microb Biotechnol* **105**, 8647–8661. https://doi.org/10.1007/s00253-021-11637-9 (2021).
24. Bajire, S. K., Prabhu, A., Bhandary, Y. P., Irfan, K. M. & Shastry, R. P. 7-Ethoxycoumarin rescued from infection of COPD derived clinical isolate *Pseudomonas aeuginosa* through virulence and biofilm inhibition via targeting Rhl and Pqs quorum sensing systems. *World J Microbiol Biotechnol* **39**, 208. https://doi.org/10.1007/s11274-023-03655-8 (2023).
25. Alteri, C. J., Himpsl, S. D., Shea, A. E. & Mobley, H. L. T. Flexible Metabolism and Suppression of Latent Enzymes Are Important for Adaptation to Diverse Environments within the Host. *J Bacteriology* **201**, e00181. https://doi.org/10.1128/JB.00181-19 (2019).
26. Mann, R., Mediati, D. G., Duggin, I. G., Harry, E. J. & Bottomley, A. L. Metabolic Adaptations of Uropathogenic in the Urinary Tract. *Frontiers Cellular Infection Microbiology* **7**, 241. https://doi.org/10.3389/fcimb.2017.00241 (2017).
27. Edwards, C. et al. Mechanisms of amino acid-mediated lifespan extension in *Caenorhabditis elegans*. *BMC Genet* **16**, 8. https://doi.org/10.1186/s12863-015-0167-2 (2015).
28. Alvarez, J., Alvarez-Illera, P., Santo-Domingo, J., Fonteriz, R. I. & Montero, M. Modeling Alzheimer's Disease in. *Biomedicines* **10**, 288. https://doi.org/10.3390/biomedicines10020288 (2022).
29. Cooper, J. F. & Van Raamsdonk, J. M. Modeling Parkinson's Disease in *C. elegans*. *J Parkinson Dis* **8**, 17–32. https://doi.org/10.3233/Jpd-171258 (2018).
30. Komura, T., Yamanaka, M., Nishimura, K., Hara, K. & Nishikawa, Y. Autofluorescence. as a noninvasive biomarker of senescence and advanced glycation end products in. *Npj Aging Mech Dis* **7**, 12. https://doi.org/10.1038/s41514-021-00061-y (2022).
31. Athar, F. & Templeman, N. M. *C. elegans* as a model organism to study female reproductive health. *Comp Biochem Phys A* **266**, 111152. https://doi.org/10.1016/j.cbpa.2022.111152(2022) (2022).
32. Pincus, Z., Mazer, T. C. & Slack, F. J. Autofluorescence as a measure of senescence in: look to red, not blue or green. *Aging -Us* **8**, 889–898. https://doi.org/10.18632/aging.100936 (2016).
33. Garsin, D. A. *et al.* A simple model host for identifying Gram-positive virulence factors. *Proc Natl Acad Sci U S A* **98**, 10892-10897, https://doi.org/10.1073/pnas.191378698 (2001).
34. Portal-Celhay, C., Bradley, E. R. & Blaser, M. J. Control of intestinal bacterial proliferation in regulation of lifespan in *Caenorhabditis elegans*. *BMC Microb* **12**, 49. https://doi.org/10.1186/1471-2180-12-49 (2012).
35. Schulenburg, H. & Felix, M. A. The Natural Biotic Environment of *Caenorhabditis elegans*. *Genetics* **206**, 55–86. https://doi.org/10.1534/genetics.116.195511 (2017).
36. Hodgkin, J., Kuwabara, P. E. & Corneliussen, B. A novel bacterial pathogen, *Microbacterium nematophilum*, induces morphological change in the nematode *C. elegans*. *Curr Biol* **10**, 1615–1618. https://doi.org/10.1016/s0960-9822(00)00867-8 (2000).

37. Schindler, A. J. & Sherwood, D. R. Morphogenesis of the *Caenorhabditis elegans* vulva. *Wiley Interdiscip Rev Dev Biol* **2**, 75–95. https://doi.org/10.1002/wdev.87 (2013).
38. Darby, C., Cosma, C. L., Thomas, J. H. & Manoil, C. Lethal paralysis of *Caenorhabditis elegans* by *Pseudomonas aeruginosa*. *Proc Natl Acad Sci U S A* **96**, 15202–15207. https://doi.org/10.1073/pnas.96.26.15202 (1999).
39. Kirienko, N. V. et al. *Pseudomonas aeruginosa* disrupts *Caenorhabditis elegans* iron homeostasis, causing a hypoxic response and death. *Cell Host Microbe* **13**, 406–416. https://doi.org/10.1016/j.chom.2013.03.003 (2013).
40. Mahajan-Miklos, S., Tan, M. W., Rahme, L. G. & Ausubel, F. M. Molecular mechanisms of bacterial virulence elucidated using a *Pseudomonas aeruginosa-Caenorhabditis elegans* pathogenesis model. *Cell* **96**, 47–56. https://doi.org/10.1016/s0092-8674(00)80958-7 (1999).
41. Tan, M. W., Mahajan-Miklos, S. & Ausubel, F. M. Killing of *Caenorhabditis elegans* by *Pseudomonas aeruginosa* used to model mammalian bacterial pathogenesis. *Proc Natl Acad Sci U S A* **96**, 715-720, https://doi.org/10.1073/pnas.96.2.715 (1999).

Acknowledgements

This research was funded in part by the National Science and Technology Council, Taiwan (Grant 113-2321-B-005-006), and the Innovation and Development Center of Sustainable Agriculture from The Featured Areas Research Center Program within the framework of the Higher Education Sprout Project by the Ministry of Education (MOE) in Taiwan. Asif Hameed acknowledges Yenepoya (Deemed to be University) for the Seed Grant (YU/Seed grant/139–2023). We thank Dr. Manjunatha Thondamal, Department of Biotechnology, GITAM School of Technology, Visakhapatnam, for providing *C. elegans* N2 strains and OP50. We also thank Ms. Krithika and Ms. Malathi for their help in optimizing protein purification and enzyme assays.

Author contributions

A.H. conceptualization, supervision, methodology, investigation, data analysis and curation, drafting original manuscript, C.C.Y. resources, investigation, data analysis and curation, K.V.S. investigation, visualization, data analysis and curation, A.P. methodology, investigation and manuscript editing, H.R.D. investigation, visualization, data analysis and curation, R.P.S. conceptualization, methodology, investigation, data analysis and curation, manuscript editing. All the authors have reviewed the manuscript.

Funding

Yenepoya (Deemed to be University), India, YU/Seed grant/139–2023; National Science and Technology Council, Taiwan, 113-2321-B-005-006

Declaration

Competing interests

The authors declare no competing interests.

Additional information

Correspondence and requests for materials should be addressed to A.H., C.-C.Y. or R.P.S.